crystallization communications

CrossMark

Frq2 from *Drosophila melanogaster*: cloning, expression, purification, crystallization and preliminary X-ray analysis

Soledad Baños-Mateos,[a]‡ **Antonio Chaves-Sanjuán,**[a] **Alicia Mansilla,**[b] **Alberto Ferrús**[b] **and María José Sánchez-Barrena**[a]*

[a]Department of Crystallography and Structural Biology, Institute of Physical Chemistry 'Rocasolano', CSIC, Serrano 119, 28006 Madrid, Spain, and [b]Department of Molecular, Cellular and Developmental Neurobiology, Institute Cajal, CSIC, Avenida Dr Arce 37, 28002 Madrid, Spain

‡ Present address: MRC-LMB, Francis Crick Avenue, Cambridge Biomedical Campus, Cambridge CB2 0QH, England.

Correspondence e-mail: xmjose@iqfr.csic.es

Drosophila melanogaster contains two calcium-binding proteins, Frq1 and Frq2, in the nervous system that control the number of synapses and the probability of release. To understand the differential function of the two proteins, whose sequence is only 5% dissimilar, the crystal structures of Frq1 and Frq2 are needed. Here, the cloning, expression, purification, crystallization and preliminary crystallographic analysis of Frq2 are presented. The full-length protein was purified using a two-step chromatographic procedure. Two different diffracting crystal forms were obtained using a progressive streak-seeding method and detergents.

1. Introduction

Ca^{2+} transients are a universal signal in biological systems and over 100 Ca^{2+}-binding proteins are known across species. These proteins can be grouped into two main classes: the high-affinity, low-capacity and the low-affinity, high-capacity families. By and large, both families make use of the EF-hand motif as the most common structural domain to coordinate Ca^{2+} (Berridge *et al.*, 2000; Ikura & Ames, 2006; Zhou *et al.*, 2013).

In nervous systems, the speed of signal transmission is largely dependent on the efficiency in Ca^{2+} dynamics at the synapse. The distinct types of Ca^{2+} signals differ spatially, temporally and in magnitude. Thus, it is not surprising that synapses exhibit a large repertoire of Ca^{2+}-binding proteins. The variety of Ca^{2+} sensors ensures the correct transduction of Ca^{2+} signals into specific changes in synaptic function. This specificity depends on three main factors: the affinity of the sensor for Ca^{2+}, their location with respect to the Ca^{2+} signals and their interaction with other proteins. Examples of Ca^{2+} sensors are calmodulin, with a role in synaptic plasticity, and synaptotagmin, which is involved in fast neurotransmission. The neuronal calcium sensor (NCS) family of proteins (also known as frequenin; Frq) are related to calmodulin and are enriched in or expressed only in the nervous system, where they have distinct roles in the regulation of neuronal function (Burgoyne & Weiss, 2001; Burgoyne *et al.*, 2004; Burgoyne, 2007). The structures of different proteins of the family are known (Ames & Lim, 2012).

Frq belongs to the high-affinity Ca^{2+}-binding class and is conserved from yeast to humans, where its orthologue is named neuronal calcium sensor-1 (NCS-1; Pongs *et al.*, 1993). In *Drosophila*, the Ca^{2+}-binding protein frequenin (Frq) exhibits a remarkable example of structural duplicity towards the same function. The gene is duplicated, *frq1* and *frq2*, although the encoded proteins, Frq1 and Frq2, are 95% identical. In addition, the sequences of these two proteins are identical throughout the 12 sequenced *Drosophila* genomes which span >40 million years of evolution (Sánchez-Gracia *et al.*, 2010). This unusual protein sequence conservation and the maintenance of a duplicated gene throughout such a long time challenge interpretation. It is hypothesized that conserved duplications result from the functional subspecialization of one of the components within the context of a more general function or expression in which both duplicates would be required (Rastogi & Liberles, 2005). *Drosophila* Frqs control Ca^{2+} levels through the $\alpha1$ voltage-gated Ca^{2+}-channel subunit encoded in the gene *cacophony* (*cac*; Dason *et al.*, 2009). The mammalian NCS-1 also controls Ca^{2+}-channel activity (Wang *et al.*, 2001; Tsujimoto *et al.*, 2002). Both *Drosophila* Frqs
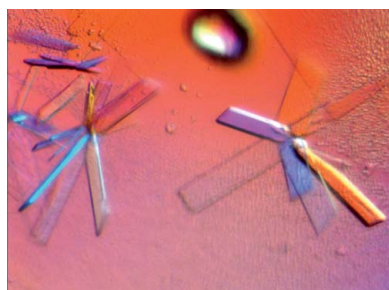
regulate neuronal probability of release and number of synapses (Romero-Pozuelo *et al.*, 2007; Dason *et al.*, 2009). The mammalian

Figure 1
Purification of Frq2. (*a*) Hydrophobic and (*b*) anion-exchange chromatography. The red and green lines represent the conductivity and the absorbance (280 nm) of the solution, respectively. (*c*) MALDI–TOF spectrum of the final purified sample. SDS–PAGE gels of the protein obtained after the hydrophobic column [inset in (*a*)] and the final crystallized sample [inset in (*c*)] are shown. Molecular-weight markers (Mw) are indicated (kDa).

NCS-1 is likely to play similar roles since it is involved in brain diseases such as autism and schizophrenia among other pathologies currently without effective treatment. Aiming to understand the subspecialization of *Drosophila frq* genes and identify structural details for target recognition, we have initiated the crystal structure solution of Frq2. Here, we report the cloning, expression, purification, crystallization and preliminary X-ray analysis of full-length Ca^{2+}-saturated and unmyristoylated Frq2 from *D. melanogaster*.

2. Materials and methods

2.1. Gene cloning, protein expression and purification

The open reading frame of *Drosophila* Frq2 was previously cloned as described by Romero-Pozuelo *et al.* (2007). A PCR fragment was amplified with the forward primer 5′-CACCATGGGCAAGAAGA-ATTCAAAATTG-3′, which included an *Nco*I site, and the reverse primer 5′-GGATCCTAATCACCACCTAAACTTAACGC-3′, with a *Bam*HI site. The PCR fragment was first cloned in the pENTR Directional TOPO vector (Life Technologies) and subsequently cloned in multiple cloning site 1 of the pETDuet-1 expression plasmid (Novagen) between *Nco*I and *Bam*HI.
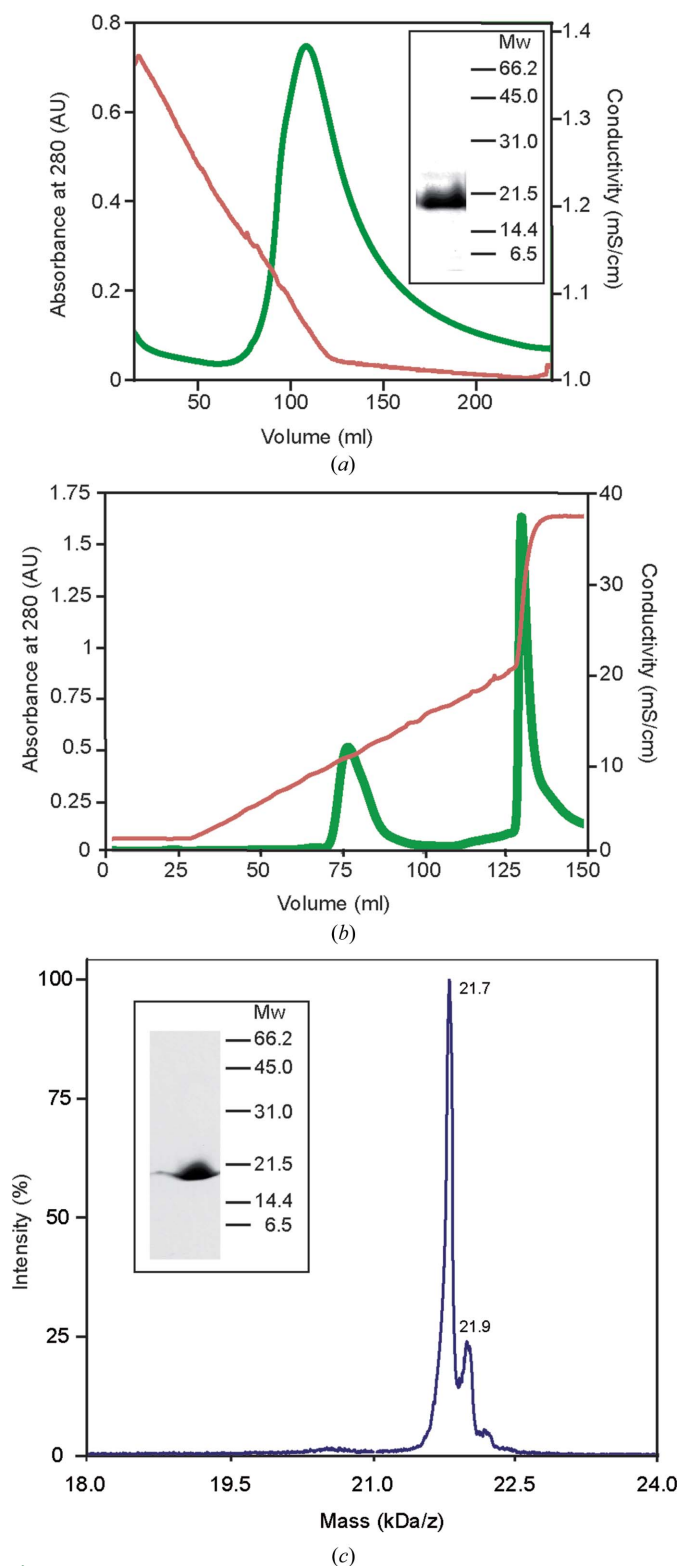
The plasmid was transformed into *Escherichia coli* BL21 (DE3) cells. The bacteria were then cultured at 310 K for 16 h in LB medium containing 100 µg ml^{-1} ampicillin. 10 ml aliquots were subcultured into 1000 ml fresh 2×TY medium plus ampicillin (100 µg ml^{-1}) and allowed to grow to an A_{600} of 0.75 at 310 K. Overnight protein expression was induced with 0.3 mM isopropyl β-D-1-thiogalacto-pyranoside (IPTG) at 289 K.

Cells were harvested by centrifugation (20 min, 1300g). The cell pellet was then resuspended in lysis buffer (50 mM HEPES pH 7.4, 100 mM KCl, 1 mM DTT) and lysed by sonication. After centrifugation (45 min, 47 808g) at 277 K, the clear supernatant was filtered (0.22 µm pore diameter), adjusted to 1 mM CaCl$_2$ and loaded onto a hydrophobic HiTrap Phenyl FF column (GE Healthcare). The column had previously been equilibrated with buffer A (20 mM Tris–HCl pH 7.9, 1 mM CaCl$_2$, 1 mM DTT). The protein was then eluted using the buffer 20 mM Tris–HCl pH 7.9, 2 mM EGTA, 1 mM DTT by decreasing the protein calcium content (Fig. 1a). Afterwards, the protein was loaded onto an ion-exchange HiTrap Q HP column (5 ml; GE Healthcare) that had previously been equilibrated with buffer A. The column was extensively washed with buffer A so that the protein was fully saturated with Ca^{2+}. A salt gradient was applied from 0 to 0.5 M NaCl. The protein eluted in two major peaks at 250 (peak 1) and 500 mM NaCl (peak 2) (Fig. 1b). The protein corresponding to peak 1, with the higher calcium content, was dialyzed against buffer consisting of 20 mM Tris–HCl pH 7.9, 50 mM NaCl, 1 mM DTT, and concentrated to 10 mg ml^{-1} using a concentrator with a 10 kDa cutoff membrane (Vivaspin). The final protein concentration was determined spectrophotometrically using a molar absorption coefficient of 19 940 M^{-1} cm^{-1} at 280 nm. The sample was aliquoted and immediately frozen at 193 K for subsequent crystallization experiments.

The final sample purity was verified by SDS–PAGE and mass spectrometry (MALDI–TOF) (Fig. 1c).

2.2. Crystallization

Preliminary crystallization conditions were established using the JBScreen Classic Kit (Jena Bioscience), Crystal Screen, Crystal Screen 2 (Hampton Research), ProPlex (Molecular Dimensions), Index (Hampton Research), SaltRX (Hampton Research) and The PACT Suite (Qiagen) with the sitting-drop vapour-diffusion method at 293 K. Drops consisting of 250 nl protein solution (10 mg ml^{-1})

and 250 nl reservoir solution were equilibrated against 65 µl reservoir solution. Condition D1 (25% PEG 4000, 0.2 M NaCl, 0.1 M HEPES pH 7.5) from ProPlex produced needle-like crystals (Fig. 2a) that did not diffract. To improve the crystal quality, various strategies were tested around this condition at 277 and 293 K.

Very thin plate-shaped crystals were grown at 277 K when the protein sample had previously been dialyzed against water. In this case, a 1 µl drop consisting of Frq2 protein solution (10 mg ml^{-1}) was mixed with reservoir solution (26% PEG 4000, 0.1 M CaCl$_2$, 0.1 M HEPES pH 7.5) in a 1:1 ratio and the mixture was equilibrated against 500 µl reservoir solution using the hanging-drop method (Fig. 2a). To increase the thickness of the crystals, progressive streak-

seeding methods were carried out (Figs. 2b, 2c, 2d and 2e). The reservoir solution PEG 4000 concentration was gradually decreased to 21% in the different seeding rounds.

Similar plate-like crystals were also obtained at 293 K from drops consisting of Frq2 solution (10 mg ml^{-1}), reservoir solution (26% PEG 4000, 0.1 M CaCl$_2$, 0.1 M HEPES pH 7.5), 0.2 M Triton X-114 (Hampton Research) in a 1:1:0.5 ratio (Fig. 2f).

2.3. X-ray analysis

Plate-like crystals obtained by streak-seeding methods at 277 K or with the use of the detergent Triton X-114 at 293 K were cryo-
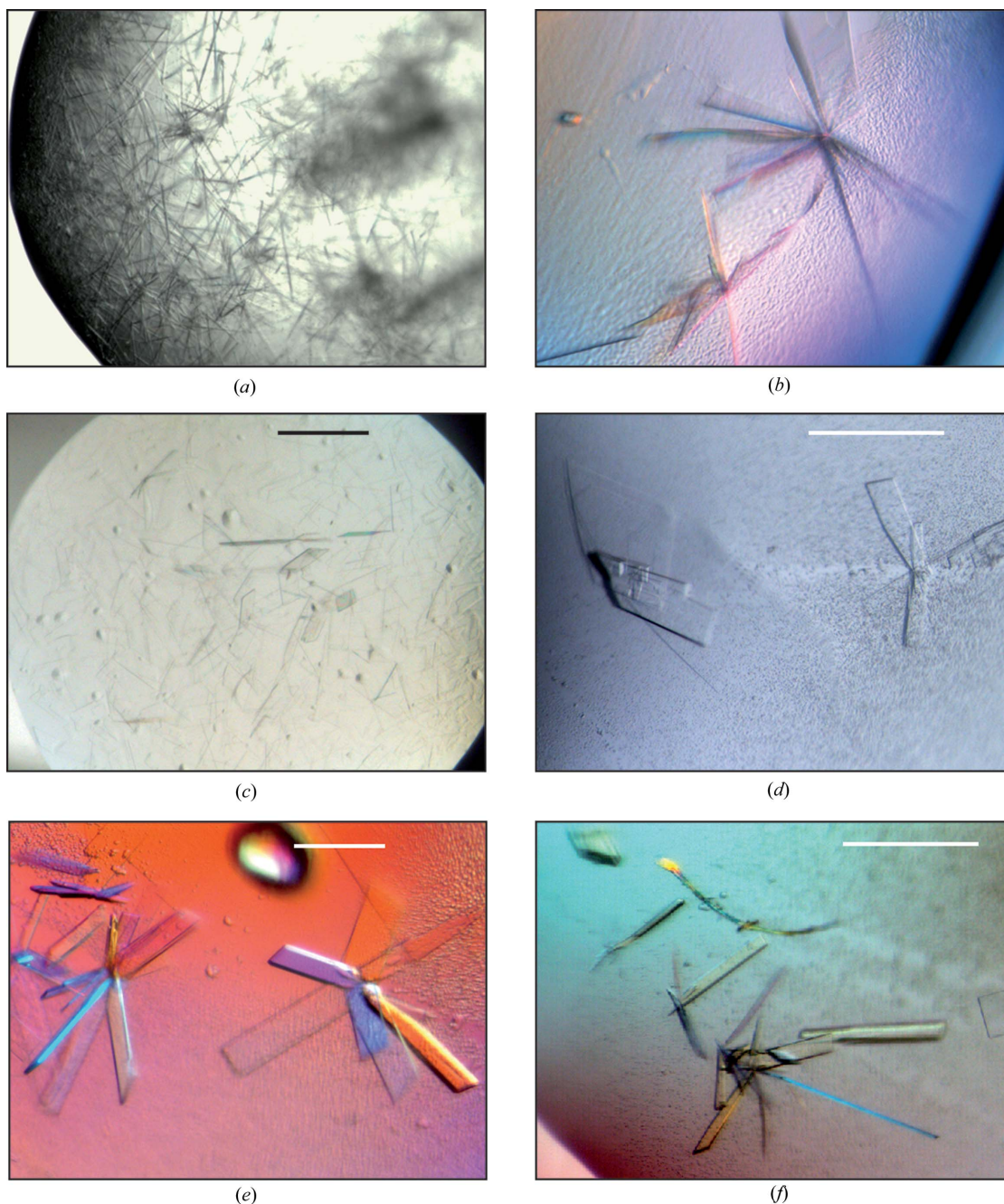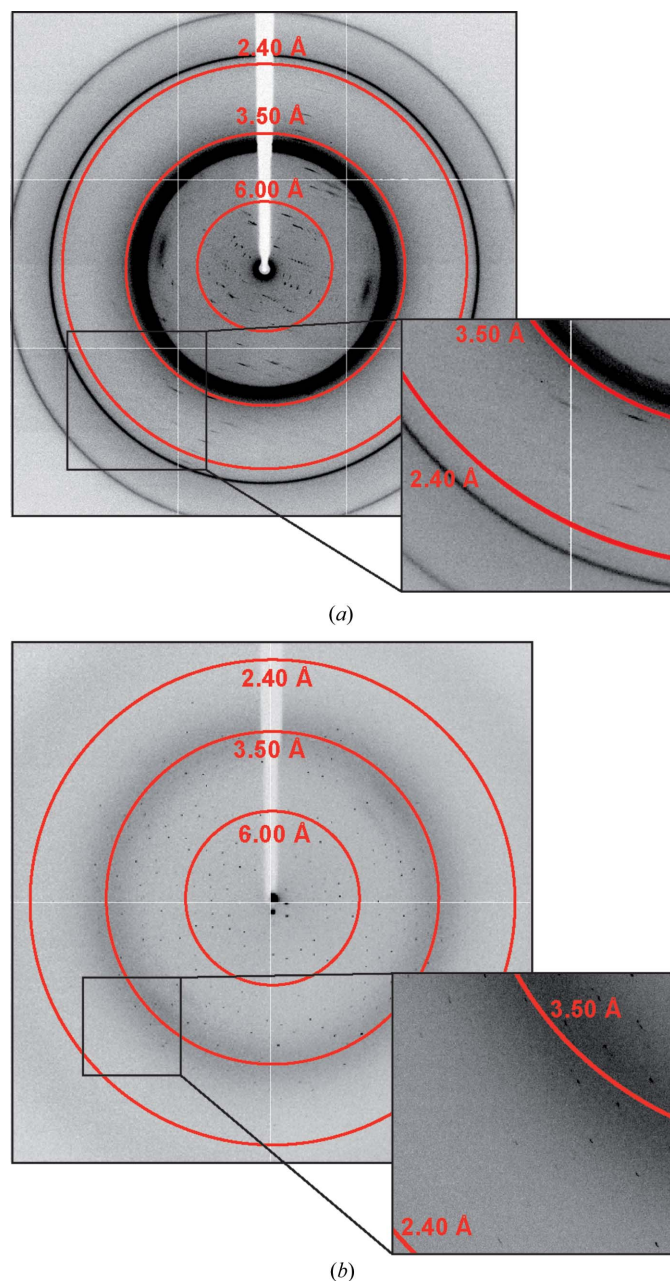

Figure 2
Crystals of Frq2. (a) Needle-like crystals obtained with commercial screens. (b) Plate-like crystals grown at 277 K. (c)–(e) Crystals obtained by progressive streak-seeding methods. Seeds from (b), (c) and (d) yielded to crystals shown in (c), (d) and (e), respectively. Final diffracting crystals are shown in (e). (f) Crystals grown in the presence of Triton X-114. Scale bars, 0.2 mm.

protected by adding 20% glycerol to their corresponding reservoir solutions. Crystals were mounted in a fibre loop and flash-cooled in liquid nitrogen for data collection. A data set was collected from each plate-like crystal at the ESRF, Grenoble (Table 1). Data were processed with *iMosflm* (Battye *et al.*, 2011) and scaled with *SCALA* (Evans, 2006). Solvent-content calculations were performed with *CCP*4 (Winn *et al.*, 2011).

3. Results and discussion

The full-length *Drosophila* Frq2 gene was cloned into a bacterial expression plasmid for protein production. The overexpressed protein was purified to homogeneity using a two-step procedure.

(a)

(b)

Figure 3
X-ray diffraction of Frq2 crystals. (*a*) Pattern of initial plate-like crystals obtained at 277 K (shown in Fig. 2*b*). (*b*) Pattern of crystals improved by progressive streak-seeding (shown in Fig. 2*e*).

Table 1
Data-collection and processing statistics.

Values in parentheses are for the highest resolution shell.

	Crystal improved by streak-seeding	Crystal improved with Triton X-114
ESRF beamline	ID14-1	ID23
Strategy	180°, $\Delta\varphi$ 0.5°	180°, $\Delta\varphi$ 0.5°
Wavelength	0.9334	0.9801
Space group	$P2_1$	$P2_12_12_1$
Unit-cell parameters		
a (Å)	55.98	52.56
b (Å)	131.19	57.57
c (Å)	56.71	128.72
α (°)	90.0	90.0
β (°)	91.1	90.0
γ (°)	90.0	90.0
Resolution limits (Å)	42.97–2.22 (2.34–2.22)	27.46–2.30 (2.42–2.30)
Solvent content (%)	45.6	45.0
Molecules in the asymmetric unit	4	2
R_{merge}	0.08 (0.47)	0.16 (0.59)
Mean $I/\sigma(I)$	12.2 (2.6)	7.9 (3.0)

Because of the high hydrophobic character of the calcium-bound Frq2, we were able to purify the protein by hydrophobic chromatography (Fig. 1*a*). Subsequent anion-exchange chromatography was used to isolate a homogeneous calcium-saturated protein sample (Fig. 1*b*). The purity of the protein was analyzed by SDS–PAGE and it was about 99% pure (Fig. 1*c*). Mass spectrometry suggested that the protein contained a mutation since the measured mass (21 756.0 ± 10.9 Da) was not coincident with the expected value (21 744.2 Da) (Fig. 1*c*). Sequencing of the pET-Duet construct verified the presence of an I178M mutation. Further analysis indicated that this change is a post-translational modification that does not alter the function of the protein (to be published elsewhere).

Non-diffracting needle-like crystals were obtained using commercial screens (Fig. 2*a*). Extensive optimization procedures yielded two different diffracting plate-like crystals that were obtained using hanging-drop vapour-diffusion techniques at 277 and 293 K. At 277 K, the crystals were extremely thin and delicate (Fig. 2*b*). They bent when mounted in the fibre loop, the quality of diffraction was low and the data could not be processed (Fig. 3*a*). Diffraction was improved (Fig. 3*b*) by producing thicker plates with progressive streak-seeding methods (Figs. 2*b*, 2*c*, 2*d* and 2*e*). Initial plates grown at 277 K were also improved at 293 K and by using the detergent Triton X-114 as an additive (Fig. 2*f*). Two data sets were collected at the ESRF, Grenoble (Table 1). Crystals grown using seeding techniques were monoclinic and those grown in the presence of Triton X-114 were orthorhombic. A summary of the X-ray diffraction data and processing statistics is shown in Table 1. To solve the crystal structure of Frq2, molecular-replacement calculations will be performed using as search models the structures of different neuronal calcium sensors (Ames & Lim, 2012).

References

Ames, J. B. & Lim, S. (2012). *Biochim. Biophys. Acta*, **1820**, 1205–1213.

crystallization communications

Battye, T. G. G., Kontogiannis, L., Johnson, O., Powell, H. R. & Leslie, A. G. W. (2011). *Acta Cryst.* D**67**, 271–281.

Berridge, M. J., Lipp, P. & Bootman, M. D. (2000). *Nature Rev. Mol. Cell Biol.* **1**, 11–21.

Burgoyne, R. D. (2007). *Nature Rev. Neurosci.* **8**, 182–193.

Burgoyne, R. D., O'Callaghan, D. W., Hasdemir, B., Haynes, L. P. & Tepikin, A. V. (2004). *Trends Neurosci.* **27**, 203–209.

Burgoyne, R. D. & Weiss, J. L. (2001). *Biochem. J.* **353**, 1–12.

Dason, J. S., Romero-Pozuelo, J., Marin, L., Iyengar, B. G., Klose, M. K., Ferrús, A. & Atwood, H. L. (2009). *J. Cell Sci.* **122**, 4109–4121.

Evans, P. (2006). *Acta Cryst.* D**62**, 72–82.

Ikura, M. & Ames, J. B. (2006). *Proc. Natl Acad. Sci. USA*, **103**, 1159–1164.

Pongs, O., Lindemeier, J., Zhu, X. R., Theil, T., Engelkamp, D., Krah-Jentgens, I., Lambrecht, H. G., Koch, K. W., Schwemer, J., Rivosecchi, R., Mallart, A., Galceran, J., Canal, I., Barbas, J. A. & Ferrús, A. (1993). *Neuron*, **11**, 15–28.

Rastogi, S. & Liberles, D. A. (2005). *BMC Evol. Biol.* **5**, 28.

Romero-Pozuelo, J., Dason, J. S., Atwood, H. L. & Ferrús, A. (2007). *Eur. J. Neurosci.* **26**, 2428–2443.

Sánchez-Gracia, A., Romero-Pozuelo, J. & Ferrús, A. (2010). *BMC Evol. Biol.* **10**, 54.

Tsujimoto, T., Jeromin, A., Saitoh, N., Roder, J. C. & Takahashi, T. (2002). *Science*, **295**, 2276–2279.

Wang, C.-Y., Yang, F., He, X., Chow, A., Du, J., Russell, J. T. & Lu, B. (2001). *Neuron*, **32**, 99–112.

Winn, M. D. *et al.* (2011). *Acta Cryst.* D**67**, 235–242.

Zhou, Y., Xue, S. & Yang, J. J. (2013). *Metallomics*, **5**, 29–42.